Molecular Microbiology (2016) 102(4), 738–751 ■
doi:10.1111/mmi.13488
First published online 27 September 2016

Thf1 interacts with PS I and stabilizes the PS I complex in *Synechococcus* sp. PCC7942

Jiao Zhan,[1] Xi Zhu,[1,2] Wei Zhou,[1,2] Hui Chen,[1] Chenliu He[1] and Qiang Wang[1]*
[1]*Key Laboratory of Algal Biology, Institute of Hydrobiology, the Chinese Academy of Sciences, Wuhan, Hubei 430072, China.*
[2]*University of the Chinese Academy of Sciences, Beijing 100039, China.*

Summary

Thylakoid formation1 protein (Thf1) is a multifunctional protein that is conserved in all photosynthetic organisms. In this study, we used the model cyanobacterium *Synechococcus* sp. PCC7942 (hereafter *Synechococcus*) to show that the level of Thf1 is altered in response to various stress conditions. Although this protein has been reported to be involved in thylakoid formation, the thylakoid membrane in the *thf1* deletion strain (ΔThf1) was not affected. Compared with the WT, ΔThf1 showed reduced PS II activity, with increased levels of D1 under high light (HL) conditions, which was resulted from blocked D1 degradation by the FtsH protease and thus inhibits PS II repair. PS I was found to be more seriously affected than PS II in ΔThf1, even under low light conditions, suggesting that PS I damage could be the primary effect of *thf1* deletion in *Synechococcus*. Further analysis revealed that the ΔThf1 mutant had a lower PS I subunit content and lower PS I stability under HL conditions. Further sucrose gradient fractionation of the membrane protein complexes and crosslinking and immunoblot analysis indicated that Thf1 interacts with PS I. Together, our results reveal that Thf1 interacts with PS I and thereby stabilizes PS I in *Synechococcus*.

Accepted 22 August, 2016. *For correspondence. E-mail wangqiang@ihb.ac.cn; Tel. (+8627) 6878 0790; Fax (+8627) 6878 0123

© 2016 John Wiley & Sons Ltd

Introduction

Oxygenic photosynthesis, the principal mechanism by which sunlight is converted into chemical energy on earth, is catalyzed by four multisubunit membrane-localized protein complexes, that is, photosystem II (PS II), the cytochrome *b*6/*f* complex, photosystem I (PS I) and ATP synthase (Hohmann-Marriott and Blankenship, 2011). The first three complexes are connected in series through the photosynthetic electron transport chain, which is coupled to proton pumping that drives ATP synthase-mediated ATP production. PS II is the core component of photosynthesis. By serving as a light-driven water plastoquinone oxidoreductase, PS II mediates the initial charge separation that generates the high energy electrons needed for photosynthetic electron transport. The PS I complex functions at the reducing end of the photosynthetic electron transfer chain as a plastocyanin-ferredoxin oxidoreductase.

The preservation and functioning of both PS I and PS II are essential for cell survival under stress conditions, including exposure to high light (HL). Both PS I and PS II are multisubunit chlorophyll (Chl)-binding protein complexes. Cyanobacterial PS I usually forms a trimer consisting of monomers composed of 11–12 subunits. By contrast, PS I in plants and algae does not form a trimer and each monomer has 3 additional subunits which are unique to plants and algae (Jordan *et al.*, 2001; Ben-Shem *et al.*, 2003). Among the PS I subunits, PsaA and PsaB form the core complex around which other subunits are organized and most cofactors of the PS I electron transfer system are bound to. The native functional form of the PS II complex appears to be a dimer, and in most detailed structural models of cyanobacterial PS II, each monomer contains 16 intrinsic and three extrinsic protein subunits (Umena *et al.*, 2011). Among the PS II subunits, the core integral subunits D1 and D2 bind most of the redox cofactors. D1 is the primary target of photooxidative damage and is rapidly degraded and replaced by de novo-synthesized subunits (Aro *et al.*, 1993, Yamamoto, 2001).

Our understanding of the functions of the different subunits of the two phototsystems has improved considerably over recent years (Nelson and Yocum, 2006).

Proteins that lack a structural function were also identified and shown to be essential regulators of photosystem assembly, stabilization and degradation; however, our knowledge of these regulatory factors is limited. One such regulatory factor, Psb29, was first identified from isolated His-tagged PS II preparations of *Synechocystis* sp PCC 6803, and a *Synechocystis* knockout lacking Psb29 has reduced PS II activity and increased uncoupling of the antenna proteins (Kashino *et al.*, 2002; Keren *et al.*, 2005). Psb29 is conserved in all oxygenic photosynthetic organisms and the homolog of Psb29 in *Arabidopsis thaliana* was named Thylakoid Formation 1 (Thf1), as it was first reported to be involved in the normal development of thylakoid membrane stacks (Wang *et al.*, 2004). In *Arabidopsis*, Thf1 was also reported to interact with GPA1 and function downstream of the plasma membrane–delimited heterotrimeric G-protein (GPA1) in the D-glucose signaling pathway (Huang *et al.*, 2006). A study of the *Triticum aestivum* (wheat) homolog of Thf1 showed that Thf1 could be isolated using the proteinaceous toxin Ptr ToxA as bait in a yeast two-hybrid screen, implying a possible role for Thf1 in the plant's response to the fungal pathogen (Manning *et al.*, 2007). Consistent with this, Thf1 in *Solanum lycopersicum* (tomato) was also reported to participate in defense against pathogen infection as a novel player in the coronatine signaling pathway (Wangdi *et al.*, 2010).

Furthermore, Thf1 was found to function in chloroplast development. Thf1 deletion in *Arabidopsis* resulted in a variegated leaf phenotype; reduced levels of FtsH protease, which repairs photodamaged D1 protein; and defects in chloroplast development (Zhang *et al.*, 2009). Consistent with this, ectopic expression of GPA1, the G protein α-subunit and mutation of Clp R4, a subunit of the ATP-dependent caseinolytic protease, resulted in increased FtsH levels and rescued the *thf1* variegation phenotype (Zhang *et al.*, 2009, Wu *et al.*, 2013). Interestingly, *thf1*-mediated leaf variegation was also reported to be triggered by defects in plastid gene expression and could be suppressed by the down-regulation of specific plastid ribosomal proteins and mutation of s-FACTOR6 (SIG6), both of which affect plastid gene expression (Hu *et al.*, 2015; Ma *et al.*, 2015).

Thf1 was also shown to affect the degradation and dynamics of Chl-protein complexes. Loss-of-function mutations in Thf1 resulted in a stay-green phenotype in both rice and *Arabidopsis*. Plants harboring a mutation in NYC4, the *Oryza sativa* (rice) ortholog of Thf1, retained relatively high levels of PS II core subunits D1 and D2, indicating that NYC4 was involved in the degradation of Chl and Chl-protein complexes during leaf senescence (Yamatani *et al.*, 2013). An analysis of a *thf1* mutant in *Arabidopsis*, which exhibits the stay-green phenotype, suggested that Thf1 modulates the dynamics of PS II-light harvesting complex II (LHCII) complexes and that the stay-green phenotype depends on the presence of both PS II and LHCII complexes (Huang *et al.*, 2013).

Thus, Thf1/Psb29 appears to be a multifunctional protein that exists in various species. However, the functions of Thf1 are poorly defined, and many of its proposed functions were deduced exclusively from morphological and physiological studies. In the present study, we used the model cyanobacterium strain *Synechococcus* sp. PCC7942 to demonstrate that the level of Thf1 increased in response to nitrogen and sulfur starvation (-N and -S), HL and low temperature stress (LT) and declined under phosphorus depletion (-P) and hyperosmotic stress (HS). By constructing and studying the *thf1* null mutant (ΔThf1) in *Synechococcus*, we show that Thf1 deletion not only limits the degradation of damaged D1 under HL conditions, but also reduces PS I stability, even under normal growth conditions. Furthermore, we demonstrate that Thf1 interacts with PS I, confirming its function on PS I.

Results

Thf1 is regulated by various stress conditions

Thf1 was found to be induced by HL conditions in *Synechocystis* and *Arabidopsis* (Wang *et al.*, 2004; Keren *et al.*, 2005). Using an antibody specific to Thf1, we examined the Thf1 protein levels under various stress conditions, including N, S and P deficiency, HS and oxidative and LT stress. We found that Thf1 was significantly induced by N and S starvation, oxidative and LT stress as well as HL conditions and inhibited by P deficiency and HS (Fig. 1).

The thylakoid membrane system is not affected in ΔThf1

To determine the function of the Thf1, we constructed targeted disruption mutants in which a kanamycin resistance cassette was introduced into the *thf1* (Synpcc7942_1555) gene of *Synechococcus* via double homologous recombination (Fig. 2A). The insertion site and full segregation of the mutant were validated by PCR analysis (Fig. 2B). We further confirmed knockout of Thf1 in the mutant by immunoblot analysis (Fig. 2B).

Thf1 was reported to be involved in thylakoid membrane formation in *Arabidopsis* by affecting vesicle transport (Wang *et al.*, 2004). Considering that light intensity can affect the ultrastructure of the thylakoid membrane (Anderson, 1986), we next evaluated whether a defect in Thf1 would affect the thylakoid

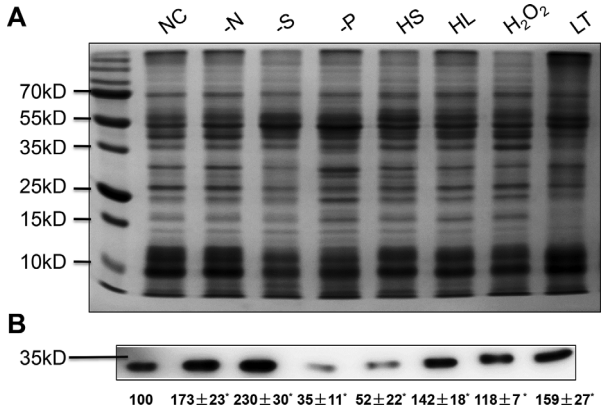

Fig. 1. Differential expression of Thf1 under various stress conditions in *Synechococcus*. The cultures were grown under normal conditions, nitrogen deficiency (-N), sulfur deficiency (-S), phosphorus deficiency (-P), cold stress (LT), HS, oxidative stress (H_2O_2) and HL stress conditions.
A. Representative image of the SDS-PAGE as the loading control in the immunoblot analysis of the current and all following figures; 10 μg of proteins from different cultures were separated by 12% SDS-PAGE and stained with Comassie Brilliant Blue.
B. Immunoblot analysis of Thf1 induction using specific antibody, relative changes were quantified using ImageJ for the current and all following figures. The 35 kD marks the location of the maker near the Thf1 protein. All data are shown as the means ± SD ($n = 5$). * indicates a significant ($P < 0.01$) difference between WT and a mutant.

membrane architecture in *Synechococcus*. To this end, we compared the thylakoid membrane ultrastructure of ΔThf1 and wild-type (WT) cells grown under different light conditions using transmission electron microscopy (TEM). Consistent with the findings of a previous study of another model cyanobacterium *Synechocystis* (Keren *et al.*, 2005), the thylakoid membrane structures of WT and ΔThf1 cells grown under low light (LL) were similar, suggesting that Thf1 was not involved in thylakoid membrane formation (Fig. 3A). However, when cells were grown under HL conditions, the number of thylakoid layers was reduced in both cell types, but to a much greater extent in ΔThf1 than in WT (Fig. 3B), suggesting that the thylakoid membrane of ΔThf1 experienced more severe oxidative stress.

Both PS I and PS II are affected by Thf1 deletion, with PS I being the initial target

To gain insight into the function of Thf1 in photosynthesis, we evaluated the growth and photosynthetic characteristics of ΔThf1 under different light conditions. Consistent with previous findings reported in *Synechocystis* (Keren *et al.*, 2005), ΔThf1 *Synechococcus* cells grew slower than WT cultures under normal light (NL) and HL conditions (Supporting Information Fig. S1B and S1C). Furthermore, the light sensitivity phenotype could be rescued by complementation with *thf1* (Supporting Information Fig. S1E and S1F), confirming that Thf1 functions in HL acclimation.

To determine the effect of Thf1 deletion on the relative contents of PS I and PS II, we conducted a low-temperature fluorescence emission spectroscopy analysis. Upon excitation at 435 nm, the emission spectrum is typically composed of three peaks, F685, F695 and F720. Among these, F685 and F695 originate from PS II, whereas F720 originates from PS I (Wang *et al.*, 2008). As shown in Fig. 4A, when grown under LL conditions, the fluorescence spectra of the WT and ΔThf1 cells were similar to each other. However, when grown at NL and HL, ΔThf1 showed decreased F720 accompanied with increased F685 and F695, as compared with those of the WT (Fig. 4B and C), although those changes in the NL were not as evident as in the HL (Fig. 4B and C). Therefore, loss of Thf1 affects the stoichiometry of PS I and PS II.

We further investigated the impact of the *thf1* deletion on the electron transport activities of PS I [from DCPIP to methyl viologen (MV)], PS II (from DPC to PPBQ) and whole chain (from H_2O to CO_2) under different light conditions. We found that the PS II activity of ΔThf1 was lower than that of the WT under HL conditions, but comparable to that of the WT under LL and NL (Fig. 4D). The apparently contradictory combination of lower PS II activity (Fig. 4D) and higher PS II titer (Fig. 4C) in ΔThf1 cells under HL conditions was consistent with

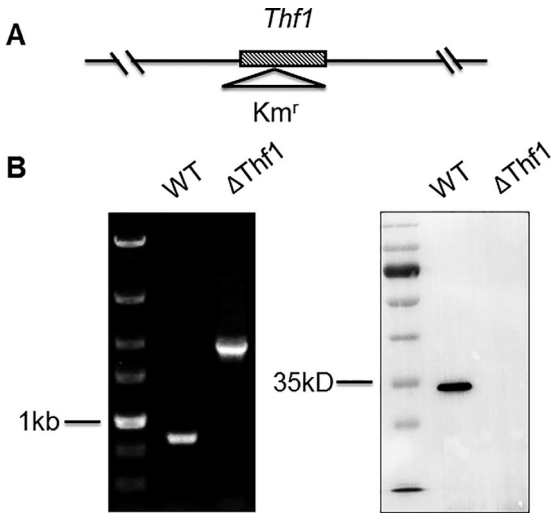

Fig. 2. Construction of the ΔThf1 mutant of *Synechococcus*.
A. Diagram showing the construction of the *thf1* mutant. The box shows the *thf1* gene (Synpcc7942_1555) of *Synechococcus*. The triangle shows the position of the kanamycin resistance cassette (Km^R).
B. Verification of the mutant. Left: PCR analysis showing fully segregation of the disrupted *thf1* gene. Right: Immunoblot analysis of WT and mutant (ΔThf1) cells using anti-Thf1 antibody.

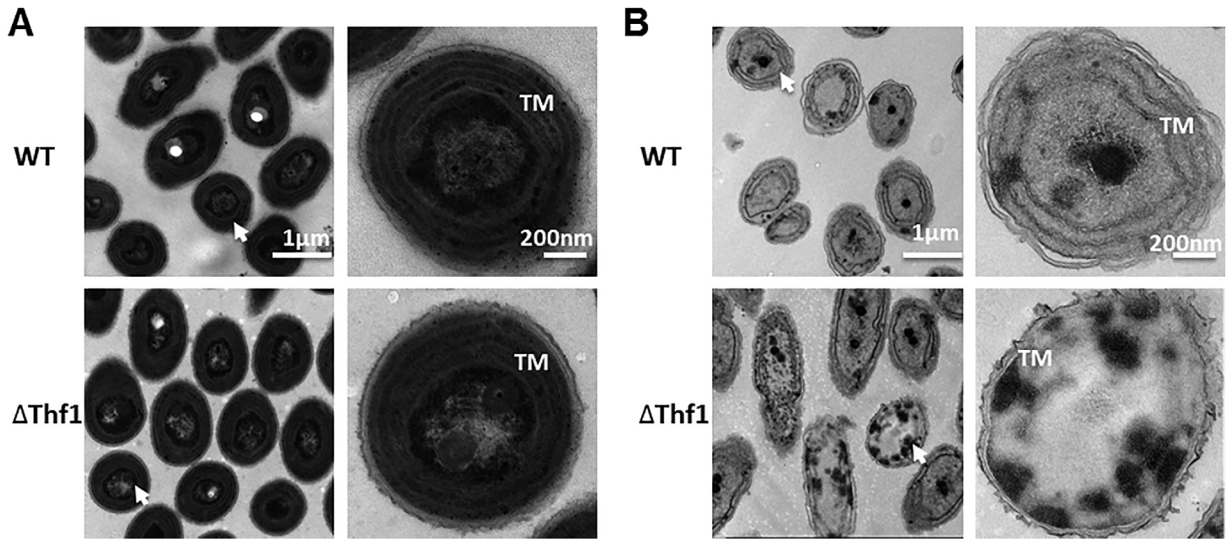

Fig. 3. Membrane architecture of WT and ΔThf1 *Synechococcus* cells grown under different light conditions.
A. Transmission electron micrographs of WT and mutant cells grown under LL conditions (7 μE).
B. Transmission electron micrographs of WT and mutant cells grown under HL conditions (HL; 1000 μE). Arrows in the right panels indicate the zoomed-in cells to their left. TM, thylakoid membrane.

findings reported in *Synechocystis* (Keren *et al.*, 2005) and it was speculated that higher PS II fluorescence in ΔThf1 was caused by increased uncoupling of PS II antenna proteins under HL conditions. As shown in Fig. 4E, the PS I activity of the mutant decreased significantly relative to the WT strain, even under LL conditions, in agreement with the results of the 77K fluorescence emission spectra (Fig. 4A–C). Although whole chain electron transport was similar between the two strains when grown under LL conditions (Fig. 4F), it was markedly lower in ΔThf1 than in the WT under NL and HL conditions.

A comparison of electron transport activities of the WT strain under different light conditions showed that PS II activity decreased, while PS I activity increased when cells were shifted from LL to NL/HL conditions (Fig. 4D and E). Furthermore, whole chain electron transport activity increased markedly with the increase in light intensity, which was synchronized with the change in PS I activity (Fig. 4E and F). These findings suggest that PS I activity is the decisive factor during HL acclimation in *Synechococcus*. Thus, the ΔThf1 mutant showed not only a relative decrease in PS II activity but also a reduction in PS I activity, with the latter being the decisive factor during HL acclimation. By contrast, the decreased PS I activity resulting from the Thf1 defect was observed even under LL conditions, suggesting that the Thf1 defect may initially affect PS I activity.

To further investigate the effects of Thf1 deletion on the photosystems during HL acclimation, PS I and PS II activity were monitored simultaneously as the cultures were transferred from LL to HL conditions. Fv/Fm, the maximum quantum efficiency of PS II photochemistry, was used as a measurement of PS II activity (Baker, 2008). While the $P700^+$ re-reduction rate in the presence of 3-(3,4-dichlorophenyl)-1,1-dimethylurea (DCMU) was used to estimate PS I activity (Yu *et al.*, 1993). Fv/Fm was similar in ΔThf1 and WT cells (Fig. 5A), but the halftime of the $P700^+$ re-reduction (*t*/2) was about 50% higher in ΔThf1 than in WT cells (Fig. 5B) before transfer to HL (0 h), indicating a similar PS II activity in both genotypes, but a reduced PS I activity in ΔThf1. After transfer to HL conditions, both strains showed decreased PS II activity as shown by decreased Fv/Fm (Fig. 5A), but increased PS I activity as shown by decreased t/2 (Fig. 5B), in correspondence to their electron transport activities (Fig. 4D and E). Furthermore, the PS II activity of ΔThf1 was only significantly lower than that of the WT after 18 hours of HL stress (Fig. 5A), but the PS I activity of ΔThf1 remained lower than that of the WT throughout the treatment (Fig. 5B). These results further confirm that loss of Thf1 initially affects PS I (Figs. 4 and 5).

D1 recovery and PS I stability are impaired by deletion of Thf1

We next conducted immunoblot analysis to examine the levels of the PS I and PS II subunits and test for further photosystem damage by Thf1 deletion under HL conditions. PsaC, PsaD and PsaE were used to estimate PS I and PsbO, CP47 and D1 were used to estimate PS II.

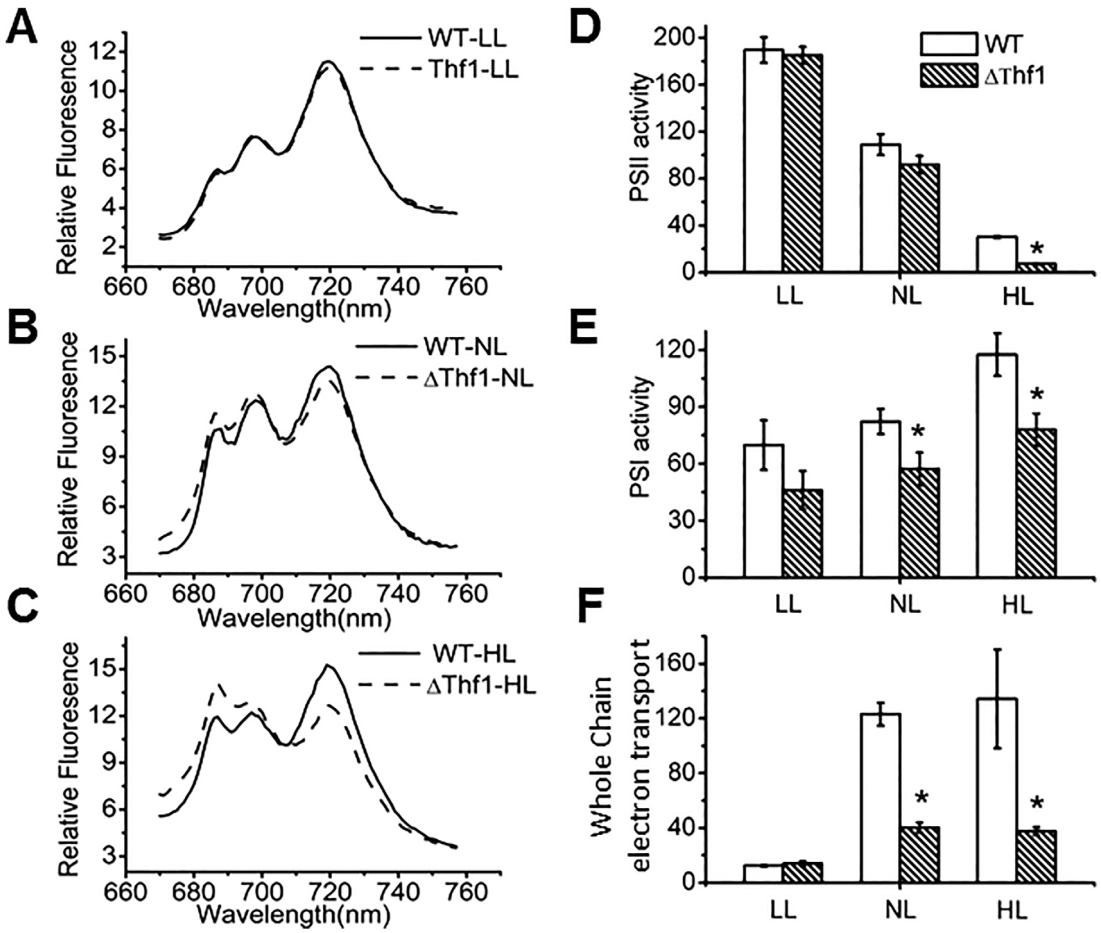

Fig. 4. The photosynthetic characteristics of WT and ΔThf1 cells grown under different light conditions. Cells were grown at LL (7 μE), NL (120 μE) and HL (1000 μE) and recovered at the mid-logarithmic growth phase for parameter determination.
A–C. 77 K fluorescence emission spectra (excitation wavelength 430 nm) of WT and ΔThf1 under different light conditions. Curves were normalized at 760 nm.
D–F. Determination of PS II (D), PS I (E) and the whole chain (F) electron transport activity. All error bars represent SD ($n = 5$). ∗ indicates a significant ($P < 0.01$) difference between WT and a mutant.

In consistent with the activity tests (Figs. 4 and 5), Fig. 6 shows that although both the WT and ΔThf1 strains had reduced level of PS I subunits under HL conditions, the ΔThf1 cells had significantly lower PS I subunits contents than the WT under NL/HL.

To figure out if PS I trimerization has any role in compensatory mechanism in regulating the PS I/PS II ratio, we analyzed the transcriptional level of *psaL* in WT and ΔThf1 under different light conditions by real-time PCR, and further analyzed the PS I trimerization in WT and ΔThf1 under HL using sucrose gradient ultracentrifugation. The qRT–PCR analysis showed that although the levels of the *psaL* mRNA were inhibited by HL, there was no significant difference between the two strains (Supporting Information Fig. S2A). The results were further proved by sucrose gradient ultra-centrifugation analysis, which showed that the content of PS I trimers (F3) were not affected by *thf1* deletion (Supporting Information Fig S2B). The results indicated that the decrease of PS I/PS II ratio caused by Thf1 defect showed no significant effect on the PS I trimerization.

While the immunoblot analysis of PS II subunits showed that although reduced with increased irradiance, the two strains had similar amounts of CP43 and PsbO under LL/NL/HL (Fig. 6). However, the amount of D1 increased significantly in ΔThf1 when cells were shifted from LL to NL/HL (Fig. 6), in contrast to those in WT, which decreased.

FtsH protease was shown to be involved in D1 degradation (Lindahl *et al.*, 2000), and the deletion of Thf1 in *Arabidopsis* resulted in a decrease in FtsH2/5 by reducing the stability of FtsH2/5 (Zhang *et al.*, 2009). As could be seen in Fig. 7, the protease FtsH could be induced by elevated irradiance at both the protein (Fig. 7A) and the mRNA levels (Fig. 7B). As compared with the WT, the FtsH protein levels were significantly declined (Fig.

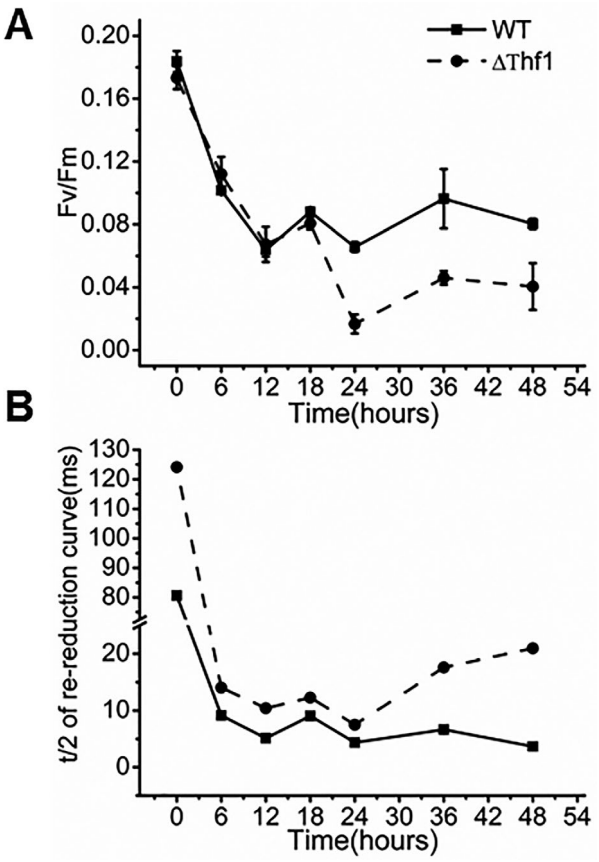

Fig. 5. Changes in PS II and PS I activity of WT and ΔThf1 during HL treatment. Samples were recovered at 0, 6, 12, 18, 24, 36 and 48 h after the transfer to HL (1000 μE), Fv/Fm (A) and the decay halftime (*t*/2) of $P700^+$ re-reduction (B) were measured and calculated to represent PS II and PS I activity, respectively. Error bars represent SD ($n = 5$). The inset panel in figure B shows representative kinetics of P700+ re-reduction curve.

7A and B) in ΔThf1, though the mRNA levels (Fig. 7B) in both strains tend to be similar under all light conditions. The findings strongly suggested that the accumulated D1 in ΔThf1 under NL/HL (Fig. 6A) were resulted from the decrease of FtsH. Taken together, it could be concluded that the deficiency of Thf1 leads to a decrease in the amount of PS I subunits, but has no effect on PS II subunits except D1.

To discriminate whether the decrease in PS I subunits of ΔThf1 under HL conditions was caused by lowered stability or downregulated synthesis of proteins, we conducted immunoblot analysis of the PS I subunits PsaC and PsaD under HL with the addition of protein synthesis inhibitor chloramphenicol (CAP; Naver *et al.*, 2001). As shown in Fig. 8, in contrast to the relatively stable PS I subunits content in WT cells during the 24 h of HL treatment in the presence of CAP, that of ΔThf1 showed significant decrease of both PsaC and PsaD. Thus, Thf1 appears to affect the stability of PS I subunits, rather than protein synthesis, during HL acclimation.

Since Thf1 could be induced by LT stress and influenced PS I stability (Figs. 1 and 8), we next examined the chilling stress acclimation of WT and ΔThf1 cells. It has been reported that PS I is an important target of photodamage in vivo under relatively weak light and chilling temperature, conditions under which PS II is not appreciably affected (Zak and Pakrasi, 2000). To avoid the PS II damage caused by higher irradiance, the chilling stress (20°C) experiment was performed under LL conditions (7 μE). As shown in Fig. 9A, ΔThf1 showed a retarded growth rate compared with the WT, accompanied with reduced PS I activity shown by higher t/2 of PS I re-reduction (Fig. 9B), while the maximum quantum efficiency of PS II photochemistry, Fv/Fm was the same in the two strains. Further westernblot analysis of PsaD indicated lower amount of PS I subunit in ΔThf1 than in WT cells (Fig. 9C).

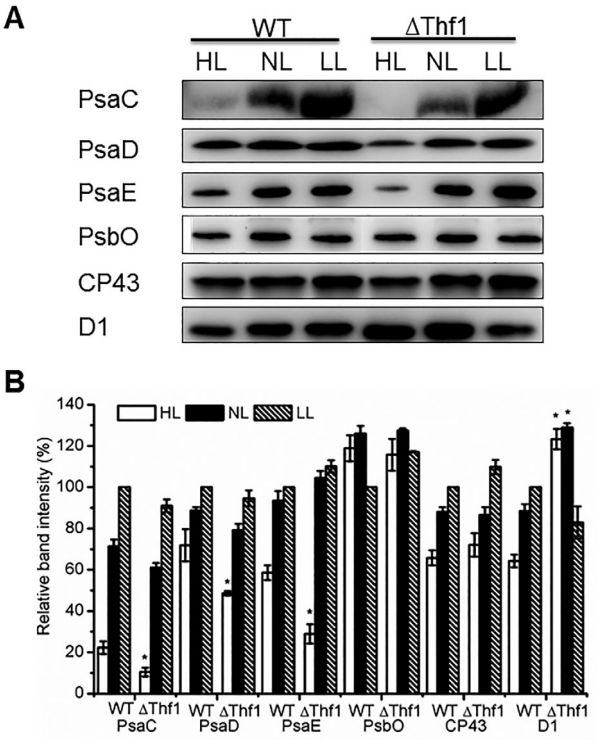

Fig. 6. The levels of PS I/PS II subunit in WT and ΔThf1 cells grown under different light conditions.
A. Immunoblot analysis of PS I subunits (PsaC, PsaD and PsaE) and PS II subunits (CP43, PsbO and D1) in WT and ΔThf1 cells grown under the indicated light conditions.
B. Quantification of the protein levels shown in (A). The specific protein levels of the WT and mutant cultured under the same conditions were compared and the asterisk indicates statistically significant differences between WT and ΔThf1 cells under the same condition (*$P < 0.01$).

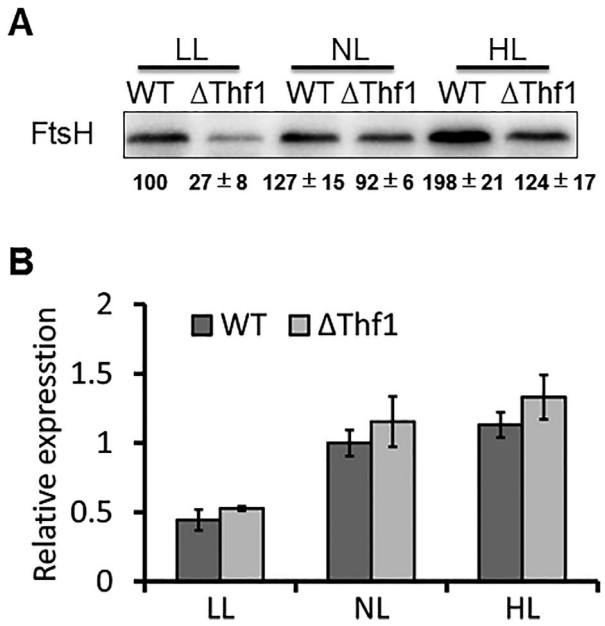

Fig. 7. Analysis of FtsH protein content and *ftsH* mRNA levels in WT and ΔThf1 cells grown under different light conditions.
A. Immunoblot analysis of FtsH protein levels in WT and ΔThf1 cells under the indicated light conditions. The data below show the quantification of the protein levels.
B. Expression of *ftsH* mRNA in WT and ΔThf1 under different light conditions were analyzed by quantitative real-time PCR. The expression level in WT cells under normal light (NL) was set to 1. Error bars represent SD ($n = 5$).

HL-induced Thf1 is localized to membrane

Arabidopsis Thf1 was reported to contain a chloroplast transit signal peptide and could be localized to both the soluble stroma and chloroplast membranes (Wang *et al.*, 2004), while the subcellular location of Thf1 in cyanobacteria remains unknown. The secondary structure of Thf1 from *Synechococcus* and two other model organisms, *Synechocystis* and *Arabidopsis*, were analyzed to determine whether they contain transfer membrane structures using Phyre (Kelley and Sternberg, 2009), JPred4 (Cole *et al.*, 2008) and GORV (Sen *et al.*, 2005). As shown in Supporting Information Figure S3, the secondary structure of Thf1 is conserved among the three organisms, and no transmembrane structures exist in any of the three proteins. Thus, Thf1 structurally appears to be water soluble.

To characterize the actual localization of Thf1 in *Synechococcus*, total (TP), membrane (MP) and soluble (SP) protein fractions were carefully prepared (see Material and Methods) and subjected to immunoblot analysis using anti-Thf1 antibody. CP43 and RbcL were used as controls of membrane protein and soluble protein, respectively. In contrast to its secondary structure (Supporting Information Fig. S3), Fig. 10A shows clearly that *Synechococcus* Thf1 could be localized to both the membrane and soluble fractions. Further test of the membrane association property of Thf1 with various potential solubilizing reagents including NaCl, Na_2CO_3, urea and TX-100 revealed that the membrane-bound Thf1 could be partially solubilized and released from the membrane by all the reagents except NaCl (Fig. 10B). This suggests that the membrane co-localized Thf1 (Fig. 10A) is peripheral membrane fraction, which tends to associate peripherally with the thylakoid, possibly through temporarily interaction instead of covalent connection.

To explore how the localization of Thf1 relates to its function, we compared the Thf1 distribution in cultures grown under LL and HL conditions by immunoblot analysis and immunofluorescence microscopy. Immunoblot analysis showed that Thf1 was localized to both the soluble and membrane fraction and could be induced significantly by HL (Fig. 11A), confirming the results of both Fig. 1 and 10A. Furthermore, as shown in Fig. 11A, the increase in the membrane fraction (204%) under HL was larger than the increase in soluble fraction (160%), indicated that the HL induced Thf1 tends to be associate with membranes, which could be further proved by in vivo localization analysis using immunofluorescence microscopy (Fig. 11B). As shown in Fig. 11B, Thf1 could be significantly induced by HL and most of the increased proteins were distributed along the cell

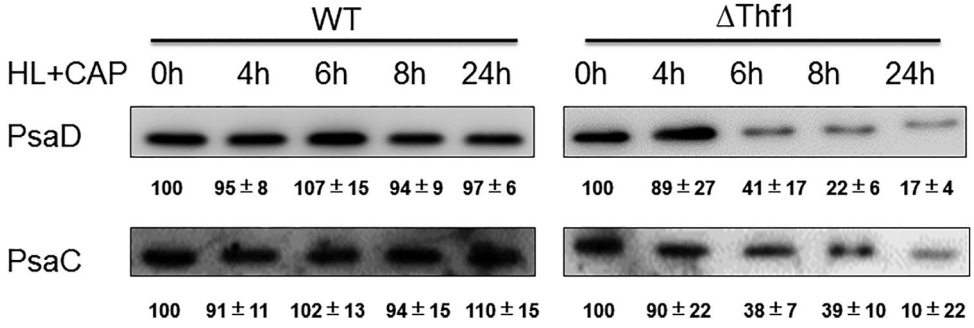

Fig. 8. Analysis of PS I stability in WT and ΔThf1 cells. Cultures were transferred to HL conditions (1000 μE) and 5 mM CAP was added to inhibit protein synthesis. Samples were recovered at 0, 4, 6, 8, 12 and 24 h and immunoblot analysis against PsaC and PsaD was performed.

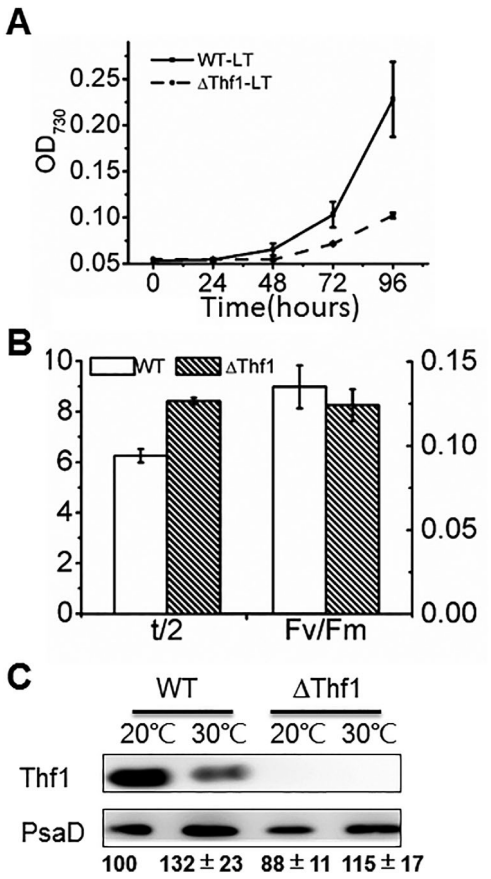

Fig. 9. Growth rates and photosynthetic competence of WT and ΔThf1 cells subjected to chilling stress.
A. Growth of WT and mutant cultures was monitored by measuring the absorption at 730 nm.
B. PS I and PS II activity of cultures under chilling stress. Half-time of $P700^+$ re-reduction and Fv/Fm were exploited to measure PS I and PS II activity, respectively.
C. Immunoblot analysis of the representative PS I subunit PsaD in total protein extracts from WT and ΔThf1 cells grown under normal temperature (30°C) and chilling stress (20°C). Error bars represent SD ($n = 5$).

membrane, consistent with the distribution of the thylakoid (Fig. 3).

Thf1 interacts with PS I

The above results showing that Thf1 was peripherally localized to membranes under HL and the loss of Thf1 was shown to affect PS I stability (Figs. 9 and 11). We thus speculated that Thf1 might be associated with the PS I complex. To explore this possibility, thylakoid membranes were isolated, solubilized in *n*-dodecyl-*b*-D-maltopyranoside (DM), fractionated by sucrose gradient separation and analyzed with Thf1 antibody. As shown in Fig. 12A, Thf1 could be detected in all three fractions, with the most abundant in F1 (the free pigment and protein fraction), suggesting that a large amount of Thf1 was released from the thylakoid by DM, in agreement with the finding that Thf1 is a peripheral membrane protein that can readily be released from the membrane by detergent treatment (Fig. 10B). We further separated F3 (the trimeric PS I fraction) by BN-PAGE and analyzed the resulting subfractions with Thf1 antibody to identify which complex Thf1 was associated with. However, Thf1 was not co-transferred with any photosystem complex (data not shown). This implies that the interaction between Thf1 and the complex was lost during electrophoresis, which in consistence with the results in Fig. 10B and proved our speculations that the association between Thf1 and the thylakoid membrane is temporarily and noncovalently. To avoid disassociation during BN-PAGE, we treated the samples with disuccinimidyl suberate (DSS), a 12-Å cross-linker that has been used to elucidate the interactions of the extrinsic proteins with photosystem proteins (Nagao *et al.*, 2010, Liu *et al.*, 2011), to "fix" the association between Thf1 and its interacting protein before sucrose gradient fractionation. F3 from ΔThf1 was used as a control. Thf1 was found to be colocalized with PS I trimers after DSS crosslinking (Fig. 12B). Taken together, these findings show that although the interaction is relatively weak, Thf1 is associated with the PS I complex, which is in agreement with its function in the PS I complex (Figs. 6 and 8).

Discussion

Psb29/Thf1 is a multifunctional protein that functions in sugar signaling, disease resistance, Chl-protein degradation and chloroplast development (Keren *et al.*, 2005, Huang *et al.*, 2006, Wangdi *et al.*, 2010). Thf1 was first identified as a substoichiometric component of His-tagged CP47 preparations isolated from *Synechocystis*

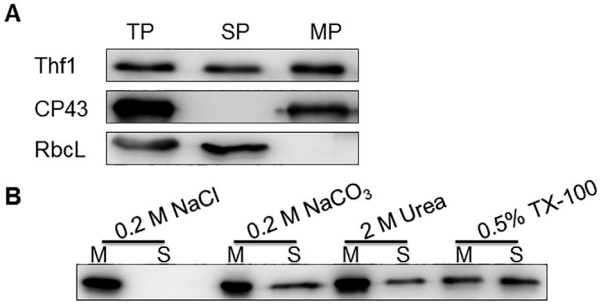

Fig. 10. Localization of Thf1 in *Synechococcus*.
A. TP, MP and SP protein fractions of *Synechococcus* were immunodecorated with the indicated antibodies. CP43 and RbcL were used as controls of membrane and soluble fractions, respectively.
B. Membrane association property of Thf1. The membrane fraction from figure A were treated with various potential solubilizing reagents as indicated, separated again into membrane (M) and soluble (S) fractions by centrifugation and subjected to immunoblot analysis.

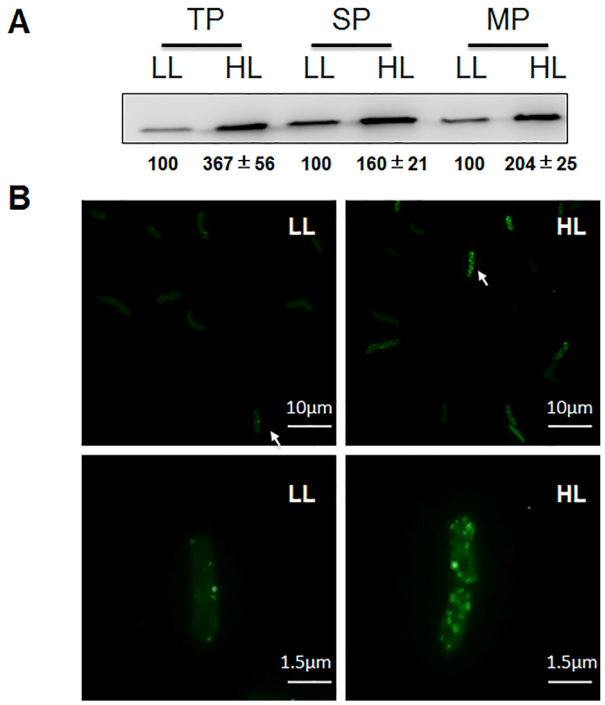

Fig. 11. Change in Thf1 localization in response to HL exposure.
A. Immunoblot analysis of Thf1 in the TP, SP and MP fractions from cultures grown under LL and HL conditions. Numbers below the blot show the relative content of Thf1.
B. Immunofluorescence images showing the adaptation of the content and the localization of Thf1 in cells grown under LL and HL. Thf1 was observed by staining cells first with anti-Thf1 antibodies and then with an Alexa Fluor® 488 Rabbit IgG Labeling Kit (Thermo Fisher Scientific) for indirect immunofluorescence microscopy. Alexa Fluor® 488 was excited with an argon laser (488 nm) and detected at 510–520 nm.

(Kashino *et al.*, 2002). Although the function of Thf1 was not well established, *thf1* knockout strains of *Arabidopsis* and *Synechocystis* were reported to have reduced PS II activity (Keren *et al.*, 2005). However, based on the results obtained in this study, *Synechococcus* Thf1 was additionally found to interact with the PS I complex and affect PS I stability in *Synechococcus*.

Thf1 was suggested to function in thylakoid membrane formation in *Arabidopsis* by affecting vesicle transport (Wang *et al.*, 2004), while in *Synechocystis*, the Thf1 defect was found to have no effect on the structure of the thylakoid membrane (Keren *et al.*, 2005). This result is confirmed by our analysis in *Synechocuccos* (Fig. 3A). However, loss of Thf1 also rendered the thylakoid membrane less stable under HL conditions (Fig. 3B).

The manner in which environmental factors regulate a protein provides clues as to its functions. As reported previously, *thf1* is induced by chilling stress and alkaline stress in the deciduous tree *Populus simonii* and *Synechocystis*, respectively (Summerfield and Sherman, 2008; Song *et al.*, 2013). In this study, we observed that Thf1 could be induced under various stresses, including -N, -S, oxidative, cold and HL stress (Fig. 1). As in *Synechocystis* (Keren *et al.*, 2005), Thf1 was found to be important for HL acclimation in *Synechoccocus* (Supporting Information Fig. S1).

During HL acclimation, a defect in Psb29 in *Synechocystis* was reported to result in a seemingly contradictory phenotype, with reduced PS II activity but higher PS II fluorescence, which was speculated to be the result of increased uncoupling of PS II antenna proteins (Keren *et al.*, 2005). This finding was confirmed in this study (Fig. 4). Furthermore, loss of Thf1 led to a defect in the breakdown of Chl and the Chl-binding protein D1 in rice and *Arabidopsis* (Huang *et al.*, 2013; Yamatani *et al.*, 2013). Consistent with this, our whole cell absorbance spectrum analysis also revealed that ΔThf1 *Synechococcus* cells had a higher Chl content than did WT cells (Supporting Information Fig. S4). It is also clear that the Chl-binding protein D1 was more abundant in ΔThf1 than in WT *Synechococcus* cells (Fig. 6). Besides, we found that ΔThf1 cells had a lower content of FtsH protein than did WT cells, but a similar level of *ftsh* mRNA expression (Fig. 7). FtsH proteases are involved in the degradation of D1 protein following photodamage to PS II (Lindahl *et al.*, 2000) and an *Arabidopsis* mutant with defects in chloroplastic FtsHs are defective in D1 degradation and PS II recovery, which results in HL sensitivity (Kato *et al.*, 2009). Taken together, these results suggest that the defect in Thf1 resulted in a decrease in FtsH content and thus in

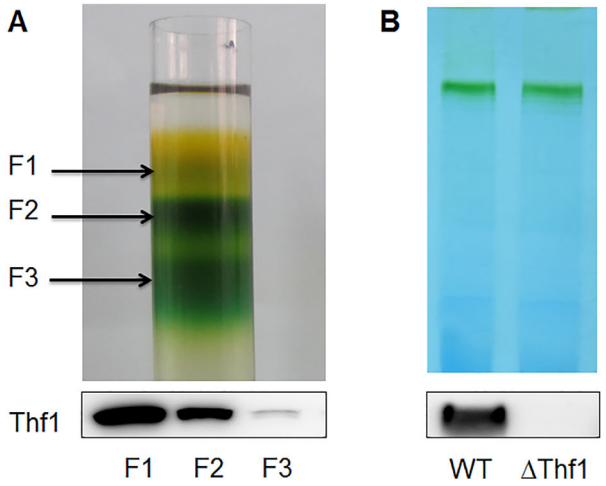

Fig. 12. The correlation between Thf1 and the photosystem.
A. Detection of Thf1 (lower panel) in the three fractions of the sucrose gradient (upper panel). The three fractions obtained from sucrose gradient ultracentrifugation are indicated with arrows as F1, F2 and F3.
B. BN-PAGE separation of DSS crosslined F3 (upper panel) and co-localization of Thf1 with PS I trimer (lower panel). Thylakoid membranes from ΔThf1 cells were subjected to the same treatment and used as the control.

inefficient degradation of damaged D1, which resulted in the accumulation of uncoupled antenna proteins, a higher Chl content, inhibition of PS II recovery and decreased PS II activity. In addition, the excitation of uncoupled antenna proteins can also lead to photosystem damage via the generation of active oxygen species (Latifi *et al*., 2009), and led to the photo-destruction of thylakoid membrane (Fig. 3B).

An important finding of our study is that, besides a decrease in PS II activity, the Thf1 defect in *Synechococcus* also repressed PS I activity and reduced the electron transport of PS I and the PS I re-reduction rate relative to the WT under HL conditions (Figs. 4 and 5). Consistent with these results, when compared with the WT, ΔThf1 cells showed a reduced PS I content, based on both the 77K fluorescence and immunoblot analysis (Figs. 4 and 6). The mechanism by which Thf1 affects the function of PS I remains to be determined. However, we demonstrated that PS I stability is reduced in the *thf1* mutant (Fig. 8). This indicates that Thf1 plays a role in stabilizing the PS I complex. The PS I assembly factor BtpA was also found to stabilize the reaction center proteins of PS I under LT, and the *btpA* knockout mutant showed a differential decrease in PS I activity and PS I content (Zak and Pakrasi, 2000). Similar to the BtpA defect, the Thf1 defect also resulted in decreased PS I activity and PS I content without affecting PS II activity under chilling stress (Fig. 9). Few protein factors involved in PS I assembly/stability have been identified in cyanobacteria, algae and higher plants. Mutations of Ycf3 led to a modest decrease in PS I content, but prevented photoautotrophic growth and caused enhanced light sensitivity (Naver *et al*., 2001). The ycf4 mutant strain of *Synechocystis* had a similar phenotype and Ycf4 was shown to be an assembly chaperone for PS I (Wilde *et al*., 1995). Inactivation of Ycf37, a conserved protein reported to affect the stability of PS I, caused a lower content of PS I and increased light sensitivity in *Synechocystis* (Wilde *et al*., 2001; Duhring *et al*., 2006). Inactivation of these genes always resulted in a reduction or complete loss of PS I reaction centers and all the corresponding mutants showed HL sensitivity, which is similar to the phenotype of Thf1 inactivation reported here. Thus, we speculate that *Synechococcus* Thf1 may affect PS I assembly. However, the mechanism remains to be deciphered. We propose that Thf1 and PS I are associated with each other, based on the presence of Thf1 in both F2 and F3 of the sucrose gradient fracitons (Fig. 12A). Furthermore, crosslinking of Thf1 by DSS revealed that Thf1 was physically associated with the PS I trimer (Fig. 12B), which confirms that Thf1 is associated with the PS I complex.

The results presented here suggest that Thf1 is involved in both PS II and PS I function. Some other thylakoid proteins showing such a two-pronged function have been identified. RpaA was reported to regulate the accumulation of monomeric PS I and D1 protein under HL conditions (Majeed *et al*., 2012). Vipp1, another protein reported to maintain the thylakoid membrane, was found to affect both photosystem activities (Gao and Xu, 2009) and reduced expression of Vipp1 in *Synchocystis* resulted in a decreased PS I content and an altered PS I/PS II ratio (Fuhrmann *et al*., 2009). Recently, Vipp1 was demonstrated to affect the biogenesis of PS I (Zhang *et al*., 2014). Interestingly, although the Thf1 defect led to both reduced PS II activity and decreased PS I activity, the latter was the decisive factor for the HL acclimation of the mutant. On one hand, the increase in whole electron transport chain activity was synchronized with the change in PS I activity (Fig. 4), and on the other, PS I damage is more harmful than PS II inhibition to photosynthetic organisms (Scheller and Haldrup, 2005; Sonoike, 2011). The recovery of PS I activity is much slower than that of PS II (Tjus *et al*., 1999) and it was reported that the photodamaged reaction center of *Arabidopsis* PS I was not completely restored after one week (Zhang and Scheller, 2004). More importantly, we suggest that the photoinhibition of PS I would enhance PS II inhibition. The cellular level of PS I is controlled to avoid excessive accumulation of the reductants produced by PS II (Melis *et al*., 1987). Once the photoinhibition of PS I is induced and electron transfer is blocked at PS I, the resulting over-reduction of the PQ pool will result in photoinhibition of PS II in the light (Sonoike, 2011). Besides, the photoinhibition of PS I would lead to the collapse of ATP synthesis, which is essential for D1 protein synthesis during the PS II repair cycle (Nixon *et al*., 2005). Thus, the decrease in PS I activity caused by the Thf1 defect enhanced PS II damage of the mutant, leading to increased sensitivity to HL. This speculation was supported by the finding that PS I activity was reduced in ΔThf1 before PS II activity was inhibited (Figs. 5 and 6).

In conclusion, by comparing the HL response of the *thf1* mutant and WT *Synechococcus*, we found that Thf1 affects not only PS II and D1 degradation by reducing the FtsH protease content, but also PS I stability. Thus, we show that Thf1 influences the stability of PS I in *Synechococcus*, thereby providing a basis for investigating the mechanism of Thf1 action.

Experimental procedures

Mutant construction

The *Synechococcus elongatus* PCC 7942 Thf1-disruption mutant was constructed by transforming WT cells with the pMD-19 (Thermo Fisher Scientific) vector carrying a *thf1*

gene that was disrupted by integration of a kanamycin resistance gene using overlap PCR technology. The upstream segment of *thf1* (primers thf1-1-F/thf1-1-R), the downstream segment of thf1 (primers thf1-2-F/thf1-2-R), and the kanamycin cassette (primers Kana-F/Kana-R) were amplified separately by PCR to generate overlapping gene segments and used as template to generate full-length disrupted *thf1*. Primers are listed in Supporting Information Table S1.

To generate strains in which the *thf1* mutation was complemented, a *NS2* targeting vector pNS2 was constructed first according to Nakahira (Nakahira *et al*., 2013). The *NS2* gene (primers NS2-F/NS2-R) was cloned and inserted into the pMD-19 vector. Next, *thf1* (primers thf1-F/thf1-R), the *cpcB* promoter (primers promoter-F/promoter-R) from *Synechocystis sp*. PCC6803 and the CAP cassette (primers Cm-F/Cm-R) were amplified by PCR using Phusion DNA polymerase as template, respectively. The DNA fragments were recombined by overlap extension PCR and the resulting fragment was cloned into the BstpI site of pNS2 to construct the *thf1* expression cassette. The constructed cassette was then transformed into the Thf1-disruption mutant.

Culture conditions

Normally, the *Synechococcus* cells were cultured under 120 μE normal light at 30°C in BG11 medium. For the stress treatment experiments, cells were harvested by centrifugation at 6,000*g* for 3 min after they had reached the mid-logarithmic growth phase (OD_{730} ~0.8), and were then cultured under different stress conditions. Deficiencies in nitrogen (N), sulfur (S) and phosphorus (P) were achieved by washing and transferring the cultures into the corresponding element-free BG11 medium. The hyperosmotic condition (HS) was achieved by adding NaCl to a final concentration of 0.5 M. Cold stress (LT) was carried out at 20°C. For the exogenous oxidative stress treatment, 1.5 mM H_2O_2 was added to the BG11 medium. The culture temperature was set to 30°C, except when samples were subjected to cold stress treatment, and normal light conditions (120 μE) were employed, except when samples were subjected to HL stress.

For the light experiments, the culture was bubbled with air under LL conditions (7 μE), NL conditions (120 μE) and HL conditions (1000 μE). Light intensities were measured using a quantum light meter (Spectrum, American). All cells were cultivated in BG-11 medium at 30°C. For chilling stress experiments, the cultures were grown at 20°C and under LL conditions. The control was grown at 30°C and under LL conditions.

77K fluorescence

77K fluorescence emission spectra were determined as described previously (Zhang *et al*., 2013) using a PTI Fluorometer (QM-4CW, Photon Technology International, South Brunswick, NJ). The logarithmic phase cell suspensions were adjusted to an OD_{730} of 0.8 in BG11 media and frozen in liquid nitrogen. An excitation wavelength of 435 nm was used to excite Chl.

Analysis of Chl fluorescence and P700 redox kinetics

Chl fluorescence was measured as described (Zhang *et al*., 2013) using a Dual-PAM-100 Chl fluorometer (Walz, Germany). The re-reduction of $P700^+$ in darkness was measured as described by Barthel (Barthel *et al*., 2013). Complete P700 oxidation was achieved by a 50-ms saturation pulse ($I = 10.000$ mmol photons m^{-2} s^{-1}), and 10 μM DCMU was added to the cultures prior to measurement. Averages of 10 individual traces were taken. $P700^+$ decay kinetics were fitted with single exponential functions to determine decay halftimes (*t*/2) using Origin 8.0.

Thylakoid membrane preparation and treatment of membranes for Thf1 localization

Thylakoid membranes were prepared as previously described (Wang *et al*., 2008; 2010). Briefly, cell pellets derived from cells grown to the mid-logarithmic phase were resuspended in ice-cold SMN buffer (50 mM MOPS, pH 7.0, 0.4 mM sucrose, 10 mM NaCl, 1 mM freshly made phenylmethylsulfonyl fluoride). Cells were broken by a French press apparatus (JN-02C, JNBIO). After removal of unbroken cells and cellular debris, the membrane suspensions were pelleted by centrifugation at 50,000*g* at 4°C for 60 min. The membranes were washed three times with SMN buffer and resuspended in SMN to 1 μg/μL Chl concentration.

Membranes were solubilized according to Schottkowski *et al*. (2009) with some modifications. Pellets obtained were resuspended in 100 μL of SMN buffer and 100 μL of 0.2 M NaCl, 0.2 M Na_2CO_3, 2 M urea, or 0.5% Triton X-100 was added. After a 30-min incubation on ice and centrifugation for 15 min at 18 000*g* at 4°C, the supernatants were collected and the pellets were washed twice with SMN buffer.

DSS cross-linking and fractionation of membrane protein complexes

DSS cross-linking experiments were performed as reported (Liu *et al*., 2011). Thylakoid membranes were resuspended at 0.2 mg/mL Chl and then incubated with 5 mM DSS for 30 min in darkness at room temperature. The cross-linking reaction was terminated by adding stop solution [Tris·Cl (pH 7.5)] to a final concentration of 50 mM for 15 min.

Membrane protein complexes were fractionated according to Wang *et al*. (2008). To fractionate the membrane protein complexes without/after crosslinking, a solution of 10% (w/v) dodecyl maltoside was added to the thylakoid membranes to achieve a detergent-to-Chl ratio of 15:1 (w:w). The membrane was solubilized at 4°C for 30 min and then loaded onto a 15–60% (w/w) continuous sucrose gradient. After centrifugation at 170,000*g* for 17 h at 4°C, the membrane was separated into three fractions, which were collected and stored at −80°C until use.

Electrophoresis and immunoblot analysis

For SDS-PAGE immunoblot analysis, proteins were extracted with 50 mM Tris-HCl (pH 7.0) and were quantitatively determined with a BCA Kit (Tiangen, China). Then, an equal amount of proteins was denatured with 10 × SDS sample buffer. Rabbit primary antibody and goat anti-rabbit secondary antibody (Sigma) were used at dilutions of 1:3,000 and 1:6,000, respectively. The hybridized proteins were detected by chemiluminescence.

Blue native PAGE was performed as described previously (Wang *et al.*, 2008). Different sucrose gradient fractions were collected and combined with a 1:10 volume of 10X sample buffer (5% Serva G; 25 mM BisTris-HCl, pH 7.0; 250 mM 6-amino-caproic acid; 10 mM EDTA; 30% sucrose). The prepared samples were then loaded onto a 5–12.5% gradient gel, and run at a constant voltage of 100 V. For immunoblot analysis, the BN gel was incubated in SDS sample buffer containing 400 mM DTT and 8% SDS for 1 h at 25°C. Immunoblot analysis and SDS PAGE were performed as described above.

Estimation of electron transport rate

The whole-chain, PS I-mediated and PS II-mediated electron transport rates were estimated by measuring the O_2 evolution/consumption using a Clark-type electrode (Hansatech, Germany) as described (Wang *et al.*, 2008; 2010). Cultures were adjusted to an $OD_{730} = 2$ with fresh BG-11 for the measurements of PS II and whole-chain electron transport. The whole-chain electron transport (H_2O to CO_2) rate was measured using water as the electron donor in the presence of 1 mM $NaHCO_3$. The PS II-mediated reaction mixture contained 5 mM NH_4Cl, 4 mM K_3FeCN and 1 mM phenyl-*p*-benzoquinone (PPBQ), which was used to measure the electron transport rate from H_2O to PPBQ via PS II. To measure the PS I-mediated electron transport rate, thylakoid membranes were isolated as above and were adjusted to a Chl concentration of 15 μg ml^{-1} with SMN buffer. PS I activity was measured as oxygen consumption in the presence of 20 μM DCMU, 2 mM NaN_3, 200 mM 2,3,5,6-tetramethyl-1,4-phenylenediamine, 5 mM sodium ascorbate and 200 mM MV.

Electron microscopy

For TEM, cells grown under LL and HL were harvested upon reaching the mid-log phase. Cells were washed three times with PBS, fixed with 2.5% glutaraldehyde and then placed in 1% OsO_4 for 2 h at room temperature. After graded ethanol dehydration, samples were embedded in Epoxy epon-812 and polymerized at 70°C for 8 h. Sections were cut, stained with both uranyl acetate and lead citrate, and examined with a Hitachi H-7000FA electron microscope.

Immunofluorescence microscopy

Microscopy analysis of cells grown in liquid BG11 medium was carried out using a confocal scanner (Zeiss LSM 710 NLO). Thf1 localization was performed as previously described (Miyagishima *et al.*, 2005). Briefly, Thf1 was observed by staining cells first with anti-Thf1 antibodies and then with an Alexa Fluor® 488 Rabbit IgG Labeling Kit (Thermo Fisher Scientific) for indirect immunofluorescence microscopy. Alexa Fluor® 488 was excited with an argon laser (488 nm) and detected at 510–520 nm.

Protein secondary structure prediction

Secondary structure prediction was carried out using the following programs: Phyre (Kelley and Sternberg, 2009), JPred4 (Cole *et al.*, 2008) and GORV (Sen *et al.*, 2005). A consensus model was constructed based on the results of all programs.

Acknowledgements

This work was supported jointly by the National Program on Key Basic Research Project (2012CB224803), the National Natural Science Foundation of China (31270094).

Conflict of Interest

The authors declare no conflict of interest.

Author contributions

QW contributed to the conception or design of the study, interpretation of the data and writing of the manuscript; JZ contributed to the acquisition, analysis, interpretation of the data; and writing of the manuscript; XZ, WZ, HC and CH contributed to the acquisition, analysis, or interpretation of the data.

References

Anderson, J.M. (1986) Photoregulation of the composition, function, and structure of thylakoid membranes. *Annu Rev Plant Physiol Plant Mol Biol* **37**: 93–136.

Aro, E.M., Virgin, I., and Andersson, B. (1993) Photoinhibition of photosystem-2 - inactivation, protein damage and turnover. *Biochim Biophys Acta* **1143**: 113–134.

Baker, N.R. (2008) Chlorophyll fluorescence: A probe of photosynthesis in vivo. *Annu Rev Plant Biol* **59**: 89–113.

Barthel, S., Bernat, G., Seidel, T., Rupprecht, E., Kahmann, U., and Schneider, D. (2013) Thylakoid membrane maturation and PSII activation are linked in greening Synechocystis sp. PCC 6803 cells. *Plant Physiol* **163**: 1037–1046.

Ben-Shem, A., Frolow, F., and Nelson, N. (2003) Crystal structure of plant photosystem I. *Nature* **426**: 630–635.

Cole, C., Barber, J.D., and Barton, G.J. (2008) The Jpred 3 secondary structure prediction server. *Nucleic Acids Res* **36**: W197–W201.

Duhring, U., Irrgang, K.D., Lunser, K., Kehr, J., and Wilde, A. (2006) Analysis of photosynthetic complexes from a

cyanobacterial ycf37 mutant. *Biochim Biophys Acta* **1757**: 3–11.

Fuhrmann, E., Gathmann, S., Rupprecht, E., Golecki, J., and Schneider, D. (2009) Thylakoid Membrane Reduction Affects the Photosystem Stoichiometry in the Cyanobacterium Synechocystis sp PCC 6803. *Plant Physiol* **149**: 735–744.

Gao, H. and Xu, X. (2009) Depletion of Vipp1 in Synechocystis sp PCC 6803 affects photosynthetic activity before the loss of thylakoid membranes. *FEMS Microbiol Lett* **292**: 63–70.

Hohmann-Marriott, M.F. and Blankenship, R.E. (2011) Evolution of photosynthesis. *Annu Rev Plant Biol* **62**: 515–548.

Hu, F., Zhu, Y., Wu, W., Xie, Y., and Huang, J. (2015) Leaf Variegation of Thylakoid Formation1 Is Suppressed by Mutations of Specific sigma-Factors in Arabidopsis. *Plant Physiol* **168**: 1066–1075.

Huang, J., Taylor, J.P., Chen, J.G., Uhrig, J.F., Schnell, D.J., Nakagawa, T., Korth, K.L., and Jones, A.M. (2006) The plastid protein THYLAKOID FORMATION1 and the plasma membrane G-protein GPA1 interact in a novel sugar-signaling mechanism in Arabidopsis. *Plant Cell* **18**: 1226–1238.

Huang, W., Chen, Q., Zhu, Y., Hu, F., Zhang, L., Ma, Z., He, Z., and Huang, J. (2013) Arabidopsis thylakoid formation 1 is a critical regulator for dynamics of PSII-LHCII complexes in leaf senescence and excess light. *Mol Plant* **6**: 1673–1691.

Jordan, P., Fromme, P., Witt, H.T., Klukas, O., Saenger, W., and Krauss, N. (2001) Three-dimensional structure of cyanobacterial photosystem I at 2.5 angstrom resolution. *Nature* **411**: 909–917.

Kashino, Y., Lauber, W.M., Carroll, J.A., Wang, Q.J., Whitmarsh, J., Satoh, K., and Pakrasi, H.B. (2002) Proteomic analysis of a highly active photosystem II preparation from the cyanobacterium Synechocystis sp PCC 6803 reveals the presence of novel polypeptides. *Biochemistry* **41**: 8004–8012.

Kato, Y., Miura, E., Ido, K., Ifuku, K., and Sakamoto, W. (2009) The variegated mutants lacking chloroplastic FtsHs are defective in D1 degradation and accumulate reactive oxygen species. *Plant Physiol* **151**: 1790–1801.

Kelley, L.A. and Sternberg, M.J.E. (2009) Protein structure prediction on the Web: A case study using the Phyre server. *Nature Protocols* **4**: 363–371.

Keren, N., Ohkawa, H., Welsh, E.A., Liberton, M., and Pakrasi, H.B. (2005) Psb29, a conserved 22-kD protein, functions in the biogenesis of Photosystem II complexes in Synechocystis and Arabidopsis. *Plant Cell* **17**: 2768–2781.

Latifi, A., Ruiz, M., and Zhang, C.C. (2009) Oxidative stress in cyanobacteria. *FEMS Microbiol Rev* **33**: 258–278.

Lindahl, M., Spetea, C., Hundal, T., Oppenheim, A.B., Adam, Z., and Andersson, B. (2000) The thylakoid FtsH protease plays a role in the light-induced turnover of the photosystem II D1 protein. *Plant Cell* **12**: 419–431.

Liu, H.J., Huang, R.Y.C., Chen, J.W., Gross, M.L., and Pakrasi, H.B. (2011) Psb27, a transiently associated protein, binds to the chlorophyll binding protein CP43 in photosystem II assembly intermediates. *Proc Natl Acad Sci USA* **108**: 18536–18541.

Ma, Z., Wu, W., Huang, W., and Huang, J. (2015) Down-regulation of specific plastid ribosomal proteins suppresses thf1 leaf variegation, implying a role of THF1 in plastid gene expression. *Photosynth Res.* **126**: 601–310.

Majeed, W., Zhang, Y., Xue, Y., Ranade, S., Blue, R.N., Wang, Q., and He, Q. (2012) RpaA regulates the accumulation of monomeric photosystem I and PsbA under high light conditions in Synechocystis sp. PCC 6803. *PloS one* **7**: e45139.

Manning, V.A., Hardison, L.K., and Ciuffetti, L.M. (2007) Ptr ToxA interacts with a chloroplast-localized protein. *Mol Plant Microbe Interact* **20**: 168–177.

Melis, A., Spangfort, M., and Andersson, B. (1987) Light-absorption and electron-transport balance between photosystem-II and photosystem-I in spinach-chloroplasts. *Photochem Photobiol* **45**: 129–136.

Miyagishima, S.Y., Wolk, C.P., and Osteryoung, K.W. (2005) Identification of cyanobacterial cell division genes by comparative and mutational analyses. *Mol Microbiol* **56**: 126–143.

Nagao, R., Suzuki, T., Okumura, A., Niikura, A., Iwai, M., Dohmae, N., *et al*. (2010) Topological analysis of the extrinsic PsbO, PsbP and PsbQ proteins in a green algal PSII complex by cross-linking with a water-soluble carbodiimide. *Plant Cell Physiol* **51**: 718–727.

Nakahira, Y., Ogawa, A., Asano, H., Oyama, T., and Tozawa, Y. (2013) Theophylline-Dependent Riboswitch as a Novel Genetic Tool for Strict Regulation of Protein Expression in Cyanobacterium Synechococcus elongatus PCC 7942. *Plant Cell Physiol* **54**: 1724–1735.

Naver, H., Bourdreau, E., and Rochaix, J.D. (2001) Functional studies of Ycf3: Its role in assembly of photosystem I and interactions with some of its subunits. *Plant Cell* **13**: 2731–2745.

Nelson, N. and Yocum, C.F. (2006) Structure and function of photosystems I and II. *Annu Rev Plant Biol* 521–565.

Nixon, P.J., Barker, M., Boehm, M., de Vries, R., and Komenda, J. (2005) FtsH-mediated repair of the photosystem II complex in response to light stress. *J Exp Botany* **56**: 357–363.

Scheller, H.V. and Haldrup, A. (2005) Photoinhibition of photosystem I. *Planta* **221**: 5–8.

Schottkowski, M., Ratke, J., Oster, U., Nowaczyk, M., and Nickelsen, J. (2009) Pitt, a novel tetratricopeptide repeat protein involved in light-dependent chlorophyll biosynthesis and thylakoid membrane biogenesis in Synechocystis sp. PCC 6803. *Mol Plant* **2**: 1289–1297.

Sen, T.Z., Jernigan, R.L., Garnier, J., and Kloczkowski, A. (2005) GOR V server for protein secondary structure prediction. *Bioinformatics* **21**: 2787–2788.

Song, Y., Chen, Q., Ci, D., and Zhang, D. (2013) Transcriptome profiling reveals differential transcript abundance in response to chilling stress in Populus simonii. *Plant Cell Rep* **32**: 1407–1425.

Sonoike, K. (2011) Photoinhibition of photosystem I. *Physiol Plant* **142**: 56–64.

Summerfield, T.C. and Sherman, L.A. (2008) Global transcriptional response of the alkali-tolerant cyanobacterium Synechocystis sp. strain PCC 6803 to a pH 10 environment. *Appl Environ Microbiol* **74**: 5276–5284.

Tjus, S.E., Moller, B.L., and Scheller, H.V. (1999) Photoinhibition of Photosystem I damages both reaction centre proteins PSI-A and PSI-B and acceptor-side located small Photosystem I polypeptides. *Photosyn Res* **61**: 303–303.

Umena, Y., Kawakami, K., Shen, J.R., and Kamiya, N. (2011) Crystal structure of oxygen-evolving photosystem II at a resolution of 1.9 A. *Nature* **473**: 55–60.

Wang, Q., Sullivan, R.W., Kight, A., Henry, R.L., Huang, J., Jones, A.M., and Korth, K.L. (2004) Deletion of the chloroplast-localized Thylakoid formation1 gene product in Arabidopsis leads to deficient thylakoid formation and variegated leaves. *Plant Physiol* **136**: 3594–3604.

Wang, Q., Jantaro, S., Lu, B., Majeed, W., Bailey, M., and He, Q. (2008) The high light-inducible polypeptides stabilize trimeric photosystem I complex under high light conditions in Synechocystis PCC 6803. *Plant Physiol* **147**: 1239–1250.

Wang, Q., Hall, C.L., Al-Adami, M.Z., and He, Q. (2010) IsiA Is Required for the Formation of Photosystem I Supercomplexes and for Efficient State Transition in Synechocystis PCC 6803. *PloS one* **5**:

Wangdi, T., Uppalapati, S.R., Nagaraj, S., Ryu, C.M., Bender, C.L., and Mysore, K.S. (2010) A role for chloroplast-localized Thylakoid Formation 1 (THF1) in bacterial speck disease development. *Plant Signal Behavior* **5**: 425–427.

Wilde, A., Hartel, H., Hubschmann, T., Hoffmann, P., Shestakov, S.V., and Borner, T. (1995) Inactivation of a Synechocystis sp strain PCC 6803 gene with homology to conserved chloroplast open reading frame −184 increases the photosystem-II to photosystem-I raion. *Plant Cell* **7**: 649–658.

Wilde, A., Lunser, K., Ossenbuhl, F., Nickelsen, J., and Borner, T. (2001) Characterization of the cyanobacterial ycf37: mutation decreases the photosystem I content. *Biochem J* **357**: 211–216.

Wu, W., Zhu, Y., Ma, Z., Sun, Y., Quan, Q., Li, P., *et al.* (2013) Proteomic evidence for genetic epistasis: ClpR4 mutations switch leaf variegation to virescence in Arabidopsis. *Plant J* **76**: 943–956.

Yamamoto, Y. (2001) Quality control of photosystem II. *Plant Cell Physiol* **42**: 121–128.

Yamatani, H., Sato, Y., Masuda, Y., Kato, Y., Morita, R., Fukunaga, K., Nagamura, Y., Nishimura, M., Sakamoto, W., Tanaka, A., Kusaba, M. (2013) NYC4, the rice ortholog of Arabidopsis THF1, is involved in the degradation of chlorophyll - protein complexes during leaf senescence. *Plant J* **74**: 652–662.

Yu, L., Zhao, J.D., Muhlenhoff, U., Bryant, D.A., and Golbeck, J.H. (1993) PsaE is required for in-vivo cyclic electron flow around photosystem-I in the cyanobacterium Synechococcus sp PCC 7002. *Plant Physiol* **103**: 171–180.

Zak, E. and Pakrasi, H.B. (2000) The BtpA protein stabilizes the reaction center proteins of photosystem I in the cyanobacterium Synechocystis sp PCC 6803 at low temperature. *Plant Physiol* **123**: 215–222.

Zhang, L., Wei, Q., Wu, W., Cheng, Y., Hu, G., Hu, F., Sun, Y ., Zhu, Y., Sakamoto, W., Huang, J. (2009) Activation of the heterotrimeric G protein alpha-subunit GPA1 suppresses the ftsh-mediated inhibition of chloroplast development in Arabidopsis. *Plant J* **58**: 1041–1053.

Zhang, S., Shen, G., Li, Z., Golbeck, J.H., and Bryant, D.A. (2014) Vipp1 is essential for the biogenesis of Photosystem I but not thylakoid membranes in Synechococcus sp. PCC 7002. *J Biol Chem* **289**: 15904–15914.

Zhang, S.P. and Scheller, H.V. (2004) Photoinhibition of photosystem I at chilling temperature and subsequent recovery in Arabidopsis thaliana. *Plant Cell Physiol* **45**: 1595–1602.

Zhang, Y.M., Chen, H., He, C.L., and Wang, Q. (2013) Nitrogen Starvation Induced Oxidative Stress in an Oil-Producing Green Alga Chlorella sorokiniana C3. *PloS one* **8**.

Supporting information

Additional supporting information may be found in the online version of this article at the publisher's web-site.